Diffusion-Weighted MR Imaging of Intracerebral Hemorrhage

Bo Kiung Kang, MD[1]
Dong Gyu Na, MD[1]
Jae Wook Ryoo, MD[1]
Hong Sik Byun, MD[1]
Hong Gee Roh, MD[1]
Yong Seon Pyeun, MD[2]

Objective: To document the signal characteristics of intracerebral hemorrhage (ICH) at evolving stages on diffusion-weighted images (DWI) by comparison with conventional MR images.

Materials and Methods: In our retrospective study, 38 patients with ICH underwent a set of imaging sequences that included DWI, T1-and T2-weighted imaging, and fluid-attenuated inversion recovery (FLAIR). In 33 and 10 patients, respectively, conventional and echo-planar T2* gradient-echo images were also obtained. According to the time interval between symptom onset and initial MRI, five stages were categorized: hyperacute (n=6); acute (n=7); early subacute (n=7); late subacute (n=10); and chronic (n=8). We investigated the signal intensity and apparent diffusion coefficient (ADC) of ICH and compared the signal intensities of hematomas at DWI and on conventional MR images.

Results: DWI showed that hematomas were hyperintense at the hyperacute and late subacute stages, and hypointense at the acute, early subacute and chronic stages. Invariably, focal hypointensity was observed within a hyperacute hematoma. At the hyperacute, acute and early subacute stages, hyperintense rims that corresponded with edema surrounding the hematoma were present. The mean ADC ratio was 0.73 at the hyperacute stage, 0.72 at the acute stage, 0.70 at the early subacute stage, 0.72 at the late subacute stage, and 2.56 at the chronic stage.

Conclusion: DWI showed that the signal intensity of an ICH may be related to both its ADC value and the magnetic susceptibility effect. In patients with acute stroke, an understanding of the characteristic features of ICH seen at DWI can be helpful in both the characterization of intracranial hemorrhagic lesions and the differentiation of hemorrhage from ischemia.

Index terms:
Brain, hemorrhage
Magnetic resonance (MR), diffusion study

Korean J Radiol 2001;2:183-191
Received April 6, 2001; accepted after revision July 13, 2001.

Department of [1]Diagnostic Radiology, Samsung Medical Center, Sungkyunkwan University School of Medicine; Department of [2]Diagnostic Radiology, Masan Samsung Hospital, Sungkyunkwan University School of Medicine

Address reprint requests to:
Dong Gyu Na, MD, Department of Radiology, Samsung Medical Center, Sungkyunkwan University School of Medicine, 50 Ilwon-dong, Kangnam-gu, Seoul 135-710, Korea.
Telephone: (822) 3410-2503
Fax: (822) 3410-0084
e-mail: dgna@smc.samsung.co.kr

The usual pattern of magnetic resonance (MR) appearances corresponding to the different stages of intracerebral hemorrhage (ICH) is well known. The generalized model for the appearance of ICH on MR images attributes the various signal intensity patterns of evolving ICH to the oxygenation state of hemoglobin and the integrity of the red blood cells (1, 2). Despite the frequent use of conventional MR imaging to evaluate the appearance and underlying biophysical basis of evolving ICH over the past few years, diffusion-weighted MR imaging (DWI) has only recently been recognized as a valuable investigative resource (3–8).

DWI is a relatively new technique which, by using additional strong diffusion-sensitizing gradients, is extremely sensitive to changes in the microscopic motion of water protons. It has proved valuable in the study of the natural history of ischemic stroke and is now a promising technique for the early detection of cerebral infarction in rou-

tine clinical practice (9–12). Although several recent studies using DWI (4–6, 8) have mainly focused on hyperacute and acute hemorrhages, its clinical reliability for differentiation between hemorrhage and infarction in hyperacute stroke has not been established. Furthermore, the various DWI features of ICH and the underlying biophysical mechanisms have not been clearly addressed.

The purposes of this study were to document the signal characteristics of various stages of ICH and to analyze the underlying mechanisms of signal change in ICH, as seen at DWI.

MATERIALS AND METHODS

Patients

This was a retrospective study of MR examinations performed in 38 patients [20 women and 18 men aged 41–86 (mean, 60.7) years] with spontaneous intracerebral hematoma unrelated to neoplasm, infarction, trauma or coagulopathy. ICH was caused by hypertension in 30 patients, ruptured aneurysm in two, and in six, the cause was not identified. The presence of intracerebral hematomas was proved by CT in 35 patients and by surgery in one; in two patients with old ICH, their presence was suggested by the findings of conventional MRI. MR studies were undertaken at various intervals after the onset of symptoms, and the five ICH stages were defined according to the duration of the interval between onset and initial MR examination. There were five stages: hyperacute (0–12 hrs; n=6), acute (13 hrs–3 days; n=7), early subacute (4–7 days; n=7), late subacute (8–30 days; n=10), and chronic (31 days or more; n=8).

MR imaging

For MR imaging, a 1.5-T scanner (Signa; GE Medical Systems, Milwaukee, Wis., U.S.A.) was used. The conventional MR imaging protocol included (a) axial T1-weighted spin-echo (467/9 [repetition time (TR) msec/echo time (TE) msec]), (b) axial T2-weighted fast spin-echo (3417/102 [effective echo time]), and (c) axial FLAIR (10000/400/2200 [inversion time]). The parameters of conventional MR imaging were a 256 ×192 matrix, a 23-cm field of view, and a 5 mm/2 mm slice thickness/intersection gap. Single-shot, spin-echo, echo-planar DWI sequences were obtained by applying diffusion gradients in three orthogonal directions at each slice, with two diffusion weightings (b value= 0 and 900 or 1000 sec/mm^2). Isotropic DWI was generated on-line by averaging three orthogonal-axis images. The

Table 1. Signal Intensities of Intracerebral Hematoma according to the Various Stages Demonstrated on MR Images in 38 Patients

Stage	Number of patients	Mean duration†	T1-weighted	T2-weighted	FLAIR	T2* gradient-echo	Diffusion-weighted
Hyperacute	6	6.0 ±3.4 (hours)	Isointense	Hyperintense	Hyperintense	Variable	Hyperintense
Acute	7	2.4 ±0.5 (days)	Isointense	Hypointense	Hypointense	Hypointense	Hypointense
Early subacute	7	5.0 ±1.0 (days)	Hyperintense	Hypo-or isointense	Hypo-or isointense	Hypo-or isointense	Hypointense
Late subacute	10	17.5 ±8.5 (days)	Hyperintense	Hyperintense	Hyperintense	Hyperintense	Hyperintense
Chronic	8	31.0 ±39.9 (months)	Iso- or hypointense	Hyper- or isointense	Variable	Iso- or hyperintense	Variable

Note.— Signal intensities were graded as hyper-, iso-, or hypointense relative to normal contralateral white matter.
†Mean duration between symptom onset and MR imaging

Table 2. Apparent Diffusion Coefficient (ADC) Value and Relative ADC of Intracerebral Hematoma according to Various Stages Demonstrated on DWI in 38 Patients

Stage	Numbers of patients	ADC value* (range)	Relative ADC (range)
Hyperacute (n=6)	6	0.54 ±0.05(0.48–0.61)	0.73 ±0.10(0.64–0.89)
Acute (n=7)	7	0.58 ±0.16(0.43–0.87)	0.72 ±0.17(0.58–1.07)
Early subacute (n=7)	7	0.55 ±0.23(0.18–0.73)	0.70 ±0.30(0.23–0.97)
Late subacute (n=10)	10	0.58 ±0.10(0.38–0.72)	0.72 ±0.16(0.46–0.97)
Chronic (n=8)	8	2.03 ±0.72(1.12–3.06)	2.56 ±0.99(1.35–3.79)

Note.— Relative ADC equals the ratio of the ADC value of hematoma to that of normal contralateral white matter.
ADC value and relative ADC were presented as means ±1 standard deviation.
*ADC value (×10^{-3} mm^2/sec)

DWI examination acquired 20 slices with parameters of 6500/96.8 (TR/TE), a 128 ×128 matrix, a 28-cm field of view, and 5-mm slice thickness with a 2-mm intersection gap. In addition, conventional T2* gradient-echo imaging (TR/TE = 450/20) was performed in 33 of the 38 patients and echo-planar T2* gradient-echo imaging (TR/TE= 1999/20) in ten.

Analysis

Two radiologists visually evaluated the signal intensities at the center and periphery of each ICH, reaching a consensus. For each MR image, the intensity at the center of a hemorrhage was visually graded as hyper-, iso-, or hypointense compared with that of normal contralateral white matter.

Quantitative analysis was used to determine the apparent diffusion coefficient (ADC) of each ICH at its center, as seen at DWI. A region of interest (ROI) was carefully placed within the hematoma and also in contralateral normal white matter. The ROI was drawn as large as possible while using a circular or rectangular ROI on the workstation, and its area ranged from 14 to 302 mm^2. In each case, one radiologist measured the ROI once. ADC values were calculated according to the formula

$$ADC=(\ln S_2 - \ln S_1)/\Delta\beta$$

where S_1=ROI signal intensity with diffusion gradients, S_2=ROI signal intensity without diffusion gradients, and $\Delta\beta$=the difference in b value between images with (β=900 or 1000 sec/mm^2) and without (β=0) diffusion-sensitizing gradients. Relative ADC, which is the ratio of the ADC value for a lesion to that for normal contralateral white matter, was also calculated in each case. All data concerning ADC values and relative ADC for each stage are presented as means ±1 standard deviation.

RESULTS

The results of the present study are summarized in Tables 1 and 2. The time course of the relative ADC is shown in Figure 1.

Hyperacute stage

In all six patients with hyperacute ICH, the signals at the center of the hematoma were hyperintense at DWI, isointense on T1-weighted images, and heterogeneously hyperintense on T2-weighted and FLAIR images. At DWI, focal marked hypointensity was seen in all patients at some portion of the hematoma, which was surrounded by a hyperintense rim. In all patients, T1-weighted imaging revealed a thin, slightly hypointense rim. On T2-weighted images, this was iso- or hypointense and was located at the periphery of the hematoma, inside the region of perilesional hyperintensity, a finding consistent with edema in adjacent parenchyma. Compared with T2-weighted images, conventional gradient-echo images showed mixed iso- or hyperintensity at the center of the hemorrhage and a more noticeable hypointense rim at its periphery. Echo-planar gradient-echo images were obtained in three of six patients and showed prominent signal loss surrounding the hematoma and heterogeneous signal intensity at its center. Mean relative ADCs at the center of a hyperacute hemorrhage and at the hyperintense rim surrounding it were 0.73 and 1.45, respectively.

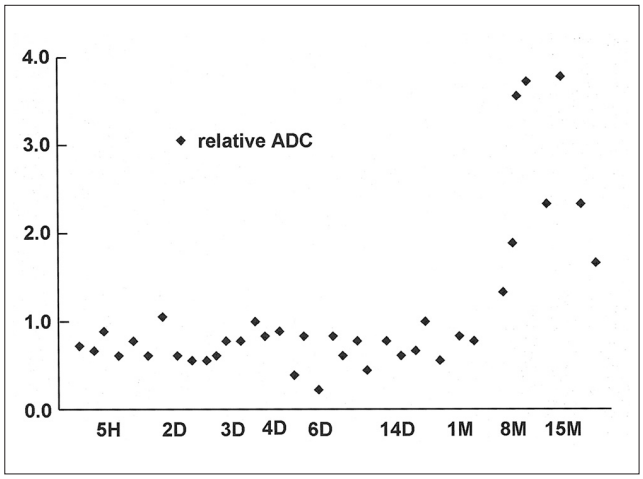

Fig. 1. The time course of relative ADC. The graph shows that in hyperacute, acute, early subacute, and late subacute hematomas, relative ADC is consistently lower than that of normal contralateral white matter. Only in chronic hematoma is relative ADC elevated.

Acute and early subacute stages

In all 14 patients whose hematomas were acute or early subacute, these appeared markedly hypointense on diffusion-weighted, T2-weighted, FLAIR, and gradient echo images (Figs. 3, 4). T1-weighted images showed the hematoma as heterogeneously isointense at the acute stage and markedly hyperintense at the early subacute stage. At both stages, DWI consistently revealed that in all these patients, a thin, markedly hyperintense rim, varying in thickness and completeness, was present at the periphery of the hematoma. The bright rims corresponded to the areas of hyperintensity seen on T2-weighted images to surround hematomas. Echo-planar gradient-echo images were obtained in five of the 14 patients with acute and early subacute ICHs. The signal intensities observed were markedly hypointense, though the hyperintense rim seen at DWI was not demonstrated. Mean relative ADCs at the center

of the hematoma were 0.72 and 0.70 at the acute and early subacute stages, respectively. In the bright rim surrounding the hemorrhage, the mean ADC was 0.98 and the mean relative ADC was 1.23.

Late subacute stage

In all ten patients with hematomas at this stage, diffusion-weighted, T1- and T2-weighted, and FLAIR images showed marked hyperintensity (Fig. 5), While gradient-echo images demonstrated heterogeneous hyperintensity. In no case was the bright rim seen at DWI at the acute and early subacute stages still visualized. The mean relative ADC at the late subacute stage was 0.72.

Chronic stage

At DWI, four of the eight chronic hematomas appeared homogeneous and markedly hypointense, and the remaining four showed an isointense center surrounded by a hy-

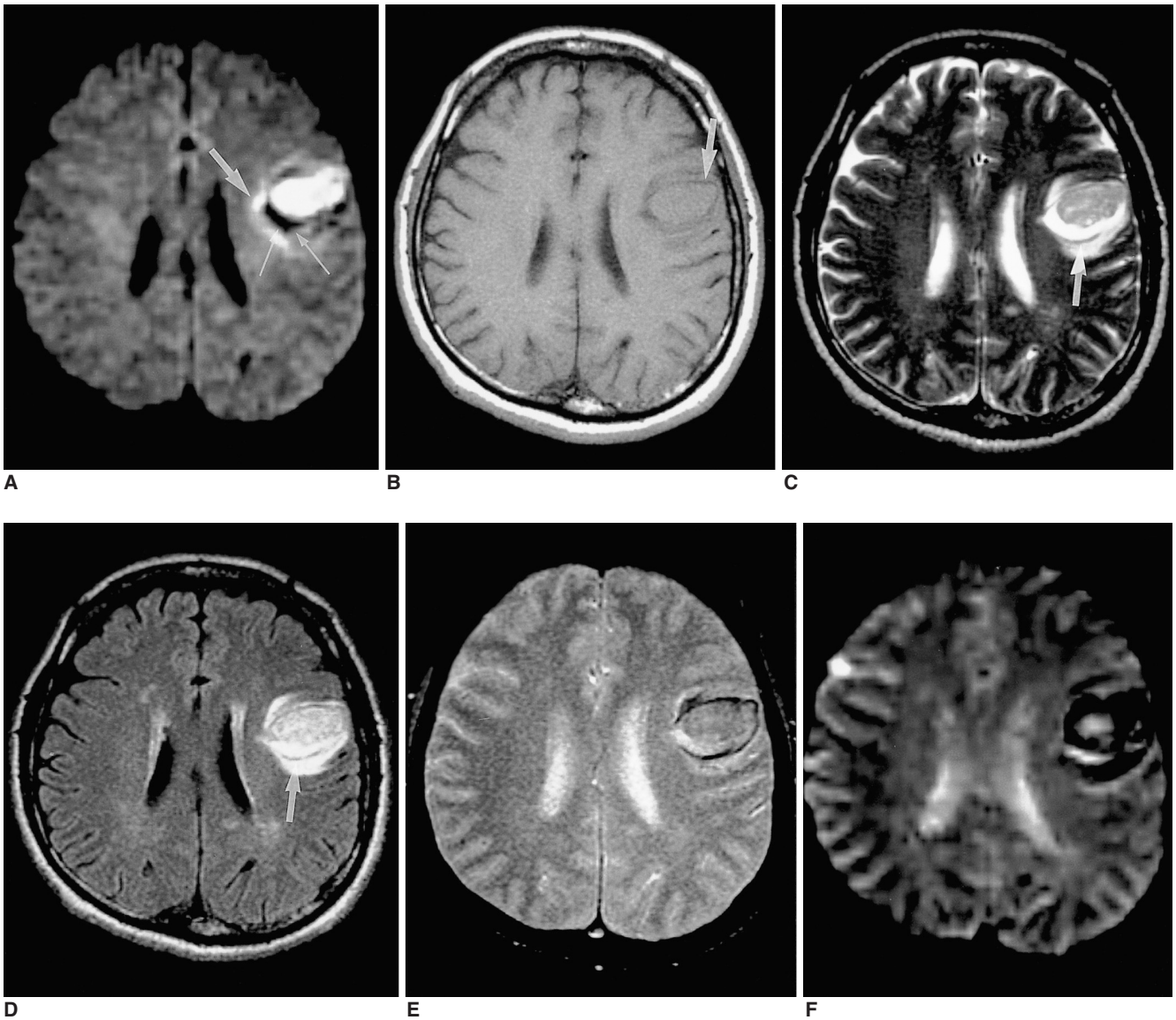

Fig. 2. A 53-year-old man with hyperacute intracerebral hematoma seen on MR images obtained 2 hours after the onset of symptoms.
A. Diffusion-weighted image shows the hematoma as hyperintense, and a peripheral focal area of marked hypointensity is observed (thin arrows). In addition, a hyperintense rim (arrow) is demonstrated around the hematoma.
B. T1-weighted image shows an isointense hematoma with a hypointense rim (arrow) in the left frontal lobe.
C, D. On T2-weighted (**C**) and FLAIR (**D**) images, the hematoma is hyperintense, and a thin hypointense rim (arrows) is seen inside the region of perilesional edema.
E, F. Conventional (**E**) and echo-planar (**F**) T2* gradient-echo images show greater signal loss around this isointense hematoma.
The focal hypointense area seen on this diffusion-weighted image does not accurately correspond to the hypointense rim seen on T2-weighted and conventional T2* gradient-echo images. The hypointense area (thin arrow) apparent at DWI corresponds to the hyperintense area seen inside the hypointense rim on the T2-weighted image, which appears to be a liquid separated from a clot.

pointense rim. On T2- weighted and gradient-echo images, a complete hypointense rim surrounded the hematoma's hyperintense center (Fig. 6). The mean relative ADC at the core of a chronic hemorrhage was 2.56.

DISCUSSION

In many clinical situations, especially those in which acute ischemic stroke is suspected, DWI has become an integral part of MRI examinations. With the advent of early management for patients with acute cerebral ischemia, it is also one of the imaging modalities of choice for the assessment of tissue viability (13, 14). Before the initiation of thrombolytic treatment or other interventions, however, an optimal treatment outcome demands accurate discrimination between ischemic and non-ischemic stroke, especially acute intracerebral hemorrhage.

It is known that a T2-weighted MR imaging finding of hyperacute hematoma is central hyperintensity accompanied by a hypointense rim (15–18). The central hyperintensity seen at T2-weighted imaging has been attributed to intracellular oxyhemoglobin and the hypointense rim to early intracellular deoxyhemoglobin at the periphery of a hematoma, which causes T2 shortening. This characteristic

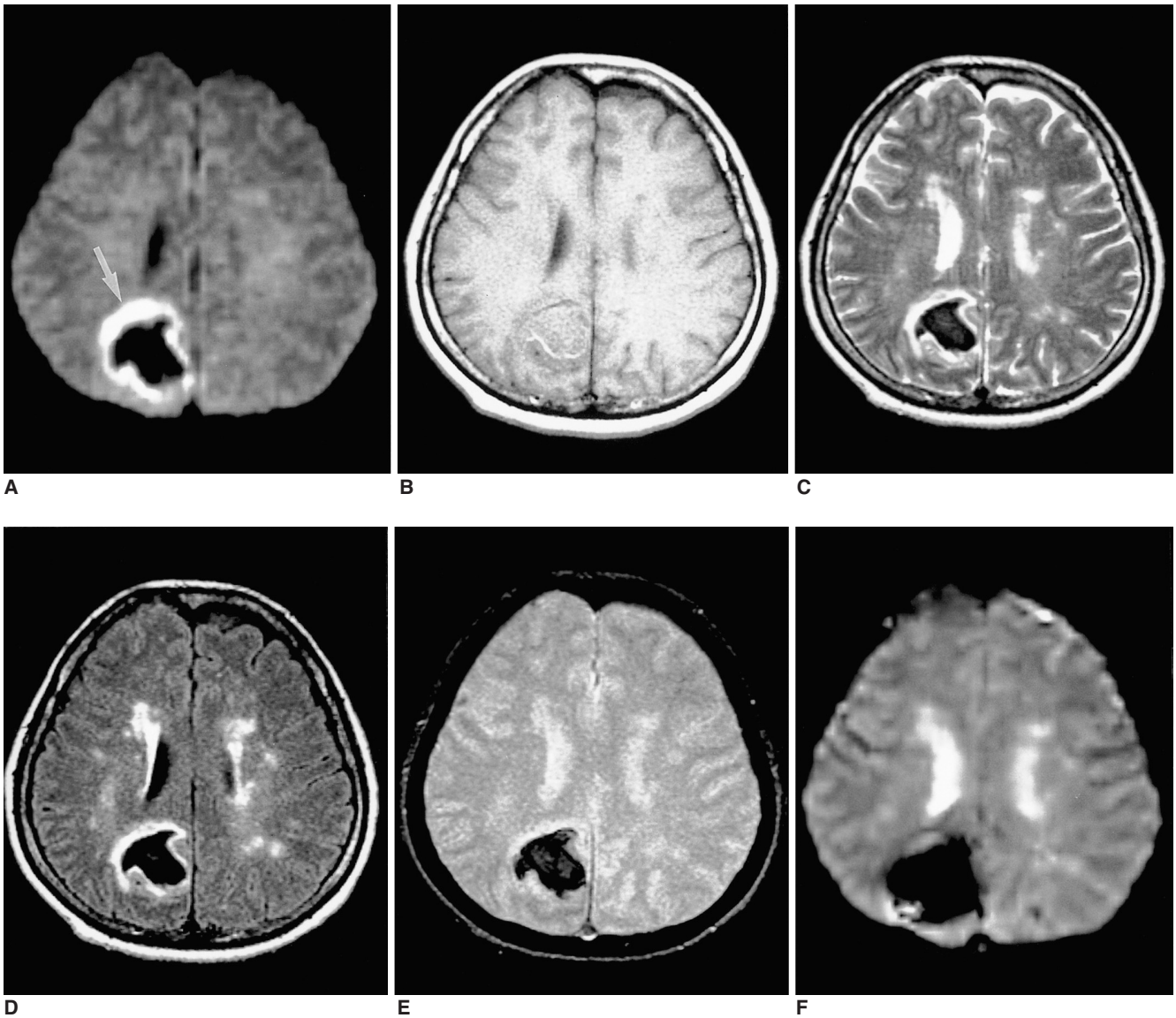

Fig. 3. A 49-year-old woman with acute intracerebral hematoma seen on MR images obtained two days after the onset of symptoms.
A. Diffusion-weighted image shows the hematoma as markedly hypointense, with a continuous rim of bright signal intensity (arrow) corresponding to the high signal area surrounding the hematoma seen on a T2-weighted image (**C**).
B. T1-weighted image shows an isointense hematoma in the right parietal lobe.
C-F. T2-weighted (**C**), FLAIR (**D**), conventional T2* gradient-echo (**E**), and echo-planar T2* gradient-echo (**F**) images depict a markedly hypointense hematoma.

hypointense rim has been reported to occur within the first few hours of hemorrhage (15−18), and in patients with acute neurologic symptoms is also valuable for differentiating between acute ischemic stroke and hemorrhage. However, because central hyperintensity is nonspecific and can also be seen in acute infarction, and the peripheral hypointense rim may not be obvious, it is often difficult to identify hyperacute hematoma using only conventional T2-weighted imaging. The peripheral hypointense rim seen in hyperacute hematoma is more obvious on conventional gradient-echo images and most prominent on EPI gradient-echo images.

In our study, the signal intensity of hyperacute ICH observed at DWI was consistent with the findings of previous studies (4−6, 8). The MR features of hyperintensity at the core of a hematoma and focal variable hypointensity were consistently found in all patients with hyperacute ICH. Hypointensity within a hyperacute hematoma, revealed by DWI, may be an important feature for differentiating hemorrhage from infarction in the practical clinical setting of hyperacute stroke, but the reliability of DWI for identifying hemorrhage has not yet been established.

The precise biophysical explanation for decreased ADC at the core of a lesion in hyperacute hematoma is uncertain. One possibility is shrinkage of extracellular space due to resorption of plasma with clot retraction (18−20), which causes high viscosity. Other possible explanations include changes in the conformation of the hemoglobin molecule (2, 6, 21) and a contraction of intact red blood cells together with decreased intracellular space (6, 22).

Previous studies have suggested that the cause of hypointensity within a hyperacute hematoma, seen on T2-

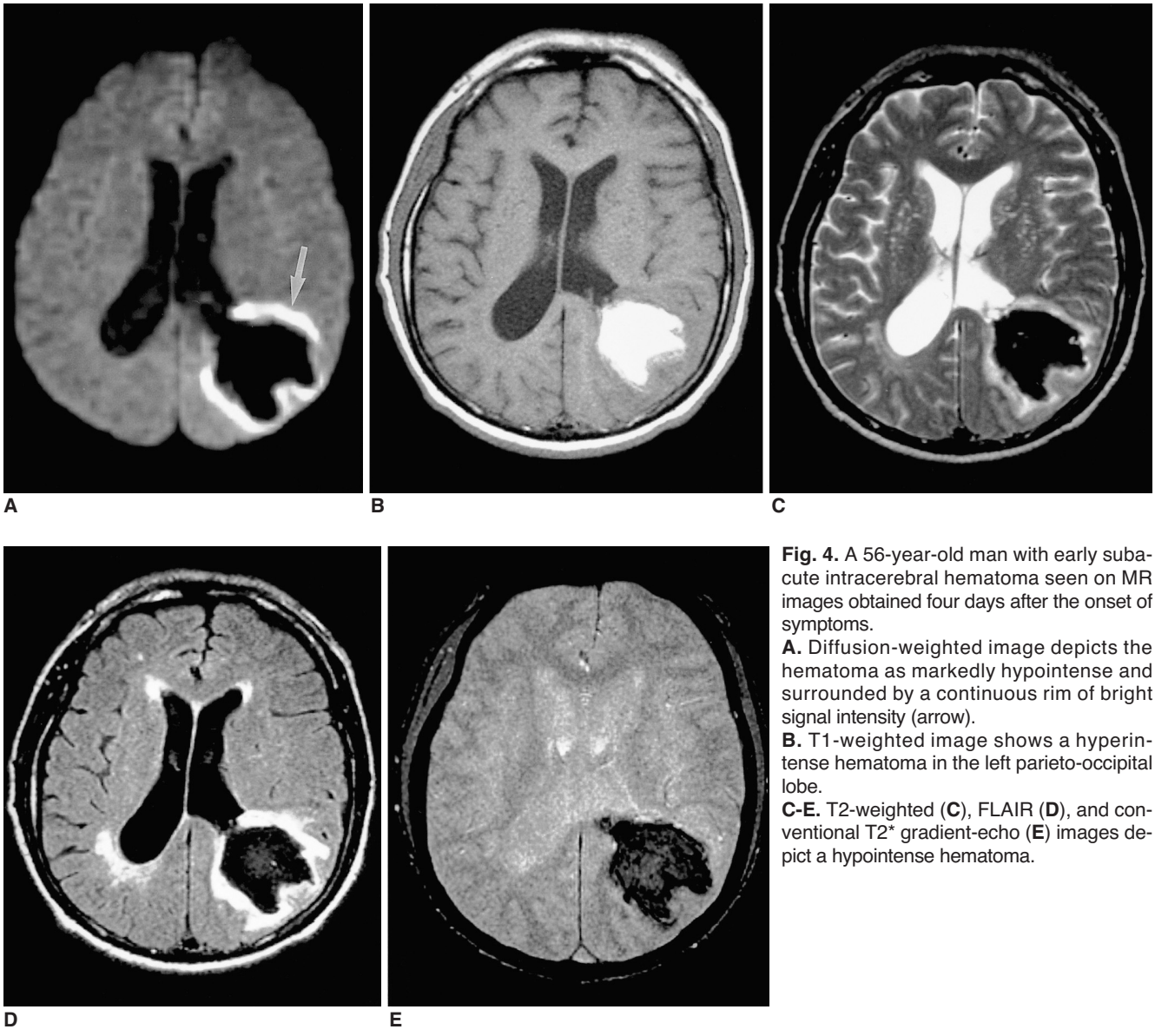

Fig. 4. A 56-year-old man with early subacute intracerebral hematoma seen on MR images obtained four days after the onset of symptoms.
A. Diffusion-weighted image depicts the hematoma as markedly hypointense and surrounded by a continuous rim of bright signal intensity (arrow).
B. T1-weighted image shows a hyperintense hematoma in the left parieto-occipital lobe.
C-E. T2-weighted (**C**), FLAIR (**D**), and conventional T2* gradient-echo (**E**) images depict a hypointense hematoma.

weighted images, may be the early presence of paramagnetic deoxyhemoglobin (4, 5, 8). The hypointense rim of hyperacute ICH seen at T2WI was more obvious on gradient-echo images with stronger susceptibility effect. However, the hypointense rim seen at DWI did not accurately correspond to that seen on T2-weighted and gradient-echo images (Fig. 2). Despite the stronger susceptibility effect, it is not certain why this is so. The focal hypointensity seen at DWI within a hyperacute hematoma might involve another causative factor: one possibility is a portion of unclotted liquid separated from a retracted clot.

In our study, the cores of lesions found in acute and early subacute hematomas were markedly hypointense at DWI as well as on T2-weighted images. This hypointensity has been attributed to the magnetic field inhomogeneity caused by paramagnetic intracellular deoxyhemoglobin in acute hematoma (1, 2, 16, 23, 24) and paramagnetic intracellular methemoglobin in early subacute hematoma (1, 23). Does et al. (25) and Schaefer et al. (26) reported that magnetic susceptibility effects caused a drop in ADC, and suggested that an accurate ADC value for acute and early subacute hematomas could not be reliably calculated. Likewise, in our study, the cores of acute and early subacute ICHs showed reduced ADC values compared with normal contralateral white matter, and , in addition, a variable, markedly hyperintense rim surrounding hyperacute, acute and early subacute hematomas was identified in all patients at DWI. Although Wiesmann et al. (8) suggested the susceptibility artifact as a possible cause of the hyperintense rim shown by DWI to surround acute and subacute hematomas, in this study such a rim was not seen on EPI gradient-echo images, which showed a stronger susceptibil-

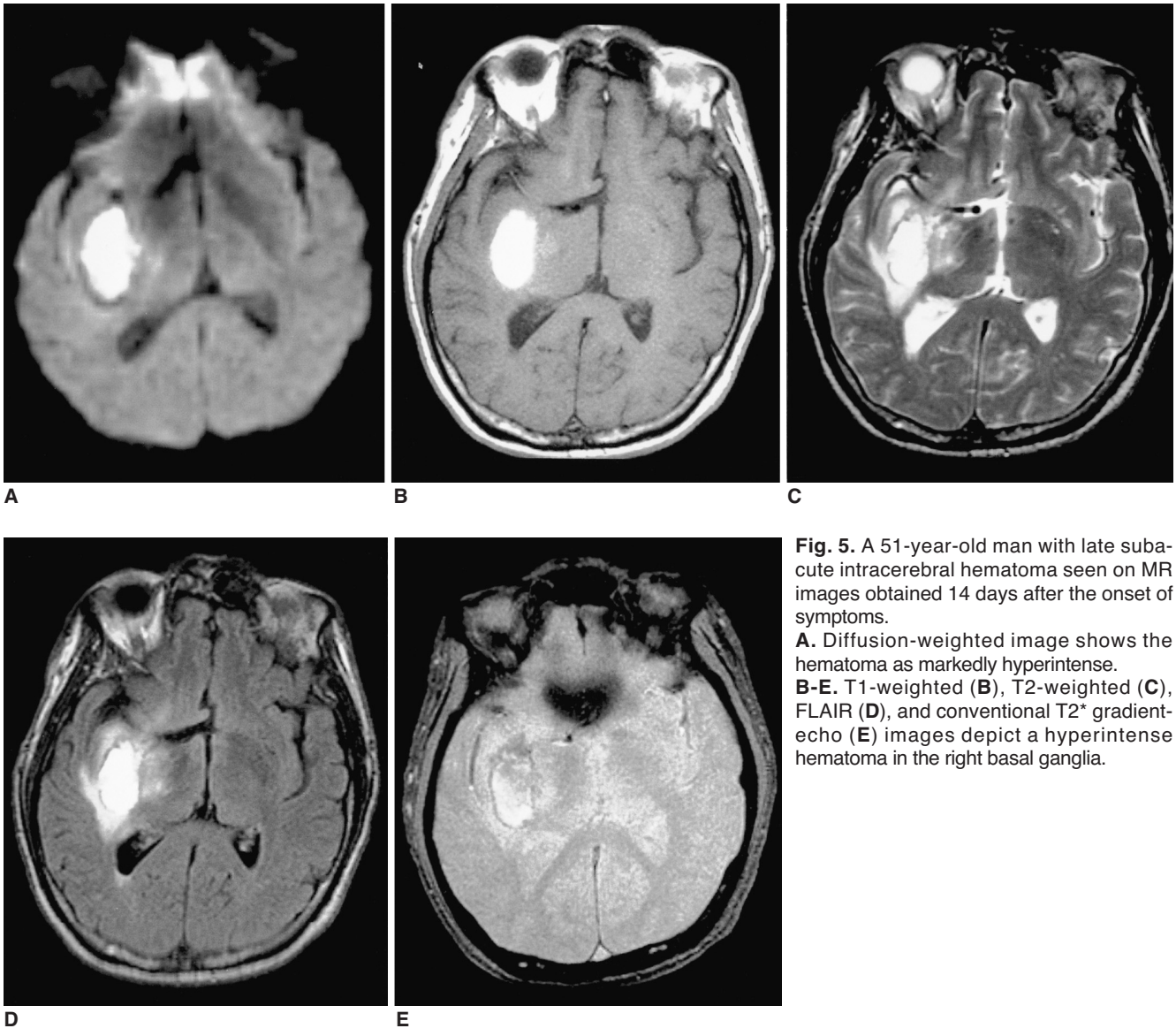

Fig. 5. A 51-year-old man with late subacute intracerebral hematoma seen on MR images obtained 14 days after the onset of symptoms.
A. Diffusion-weighted image shows the hematoma as markedly hyperintense.
B-E. T1-weighted (**B**), T2-weighted (**C**), FLAIR (**D**), and conventional T2* gradient-echo (**E**) images depict a hyperintense hematoma in the right basal ganglia.

ity effect than DWI. We believe that the rim is not caused by a susceptibility artifact due to a paramagnetic substance such as intracellular deoxyhemoglobin or methemoglobin, but may be related to the T2 shine-through effect caused by vasogenic edema surrounding the hematoma. Evidence for this is that the rim corresponded to the area of hyperintense perilesional edema seen on T2-weighted images to surround the hematomas, and that its ADC value was higher than that of normal contralateral white matter.

Our data showed that in late subacute hematoma the lesion core was hyperintense at DWI and its ADC value was lower than that of normal white matter. Atlas et al. (6) reported that the ADC value of late subacute ICH was higher than that of normal white matter, and suggested that lysis of red blood cells may lead to increased molecular diffusion. According to Ebisu et al. (3), however, relative ADC at the core of an intracerebral hemorrhage tended to remain low even at chronic stages. We believe that variations in ADC do not depend simply on whether or not red blood cell membranes are intact. At the late subacute stage of hematoma, red blood cell lysis occurs and the compartmentalization of methemoglobin is lost, resulting in the elimination of the inhomogeneous susceptibility effect (1, 2, 23). In addition, the intracellular contents are distributed in the extracellular space, possibly causing high viscosity. Other biological changes at this stage include high cellularity resulting from the infiltration of inflammatory cells and macrophages (2, 3). All these changes may affect molecular diffusion and the ADC of a hematoma. At the late subacute stage, this latter may, therefore, be related to the nature of the biological change occurring in hematomas, and during the evolution of these, ADCs appear to vary.

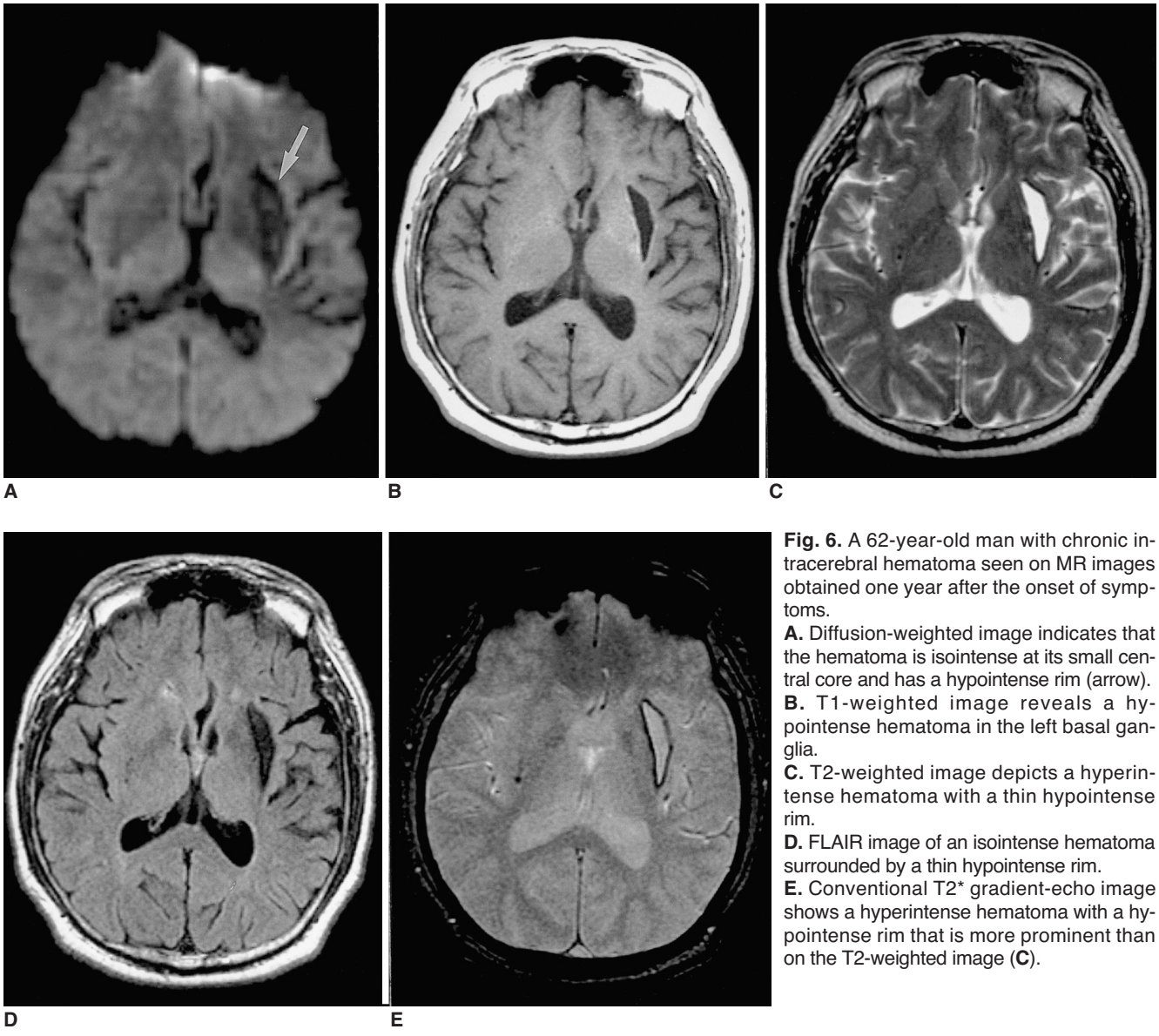

Fig. 6. A 62-year-old man with chronic intracerebral hematoma seen on MR images obtained one year after the onset of symptoms.
A. Diffusion-weighted image indicates that the hematoma is isointense at its small central core and has a hypointense rim (arrow).
B. T1-weighted image reveals a hypointense hematoma in the left basal ganglia.
C. T2-weighted image depicts a hyperintense hematoma with a thin hypointense rim.
D. FLAIR image of an isointense hematoma surrounded by a thin hypointense rim.
E. Conventional T2* gradient-echo image shows a hyperintense hematoma with a hypointense rim that is more prominent than on the T2-weighted image (**C**).

At the chronic stage of ICH, paramagnetic hemosiderin and ferritin (1, 2, 27) are found at the periphery and seen at DWI and on T2-weighted images as a dark rim surrounding the hematoma. At DWI, because the ADC value increases as the lesion approaches a cystic cavity, the lesion core of a chronic hematoma appears isointense at the early chronic stage and hypointense at the late chronic stage. In our study, all chronic hematomas were at the late chronic stage, and their ADC values were therefore higher than those of normal white matter.

The limitations of this study include the lack of histopathological confirmation and the small number of cases. Although a complete understanding of the underlying biophysical basis may require further studies with a large population, our data suggest that the appearance of intracerebral hematomas on diffusion-weighted images is influenced not only by ADC values but also by magnetic susceptibility and T2 shine-through effects. In addition, our study corroborates the key features of evolving intracerebral hematomas, as depicted by conventional MR imaging.

In conclusion, DWI demonstrated the characteristic MR features of intracerebral hematoma at various stages. We suggest that the biophysical mechanisms behind the signal changes observed at DWI are multifactorial. A better understanding of the DWI findings of intracerebral hematoma can be helpful for the differentiation of intracerebral hematoma from acute infarction and for the further characterization of intracranial hemorrhagic lesions.

References

1. Gomori JM, Grossman RI, Goldberg HI, Zimmerman RA, Bilaniuk LT. Intracranial hematomas: imaging by high-field MR. *Radiology* 1985;157:87-93
2. Bradley WG. MR appearance of hemorrhage in the brain. *Radiology* 1993;189:15-26
3. Ebisu T, Tanaka C, Umeda M, et al. Hemorrhagic and nonhemorrhagic stroke: diagnosis with diffusion-weighted and T2-weighted echo-planar MR imaging. *Radiology* 1997;203:823-828
4. Schellinger PD, Jansen O, Fiebach JB, Hacke W, Sartor K. A standardized MRI stroke protocol: comparison with CT in hyperacute intracerebral hemorrhage. *Stroke* 1999;30:765-768
5. Felber S, Auer A, Wolf C, et al. MRI characteristics of spontaneous intracerebral hemorrhage. *Radiologe* 1999;39:838-846
6. Atlas SW, DuBois P, Singer MB, Lu D. Diffusion measurements in intracranial hematomas: implications for MR imaging of acute stroke. *Am J Neuroradiol* 2000;21:1190-1194
7. Carhuapoma JR, Wang PY, Beauchamp NJ, et al. Diffusion-weighted MRI and proton MR spectroscopic imaging in the study of secondary neuronal injury after intracerebral hemorrhage. *Stroke* 2000;31:726-732
8. Wiesmann M, Mayer TE, Yousry I, Hamann GF, Bruckmann H. Detection of hyperacute parenchymal hemorrhage of the brain using echo-planar T2* -weighted and diffusion-weighted MRI. *Eur Radiol* 2001;11:849-853
9. Moseley ME, Cohen Y, Mintorovitch J, et al. Early detection of regional cerebral ischemia in cats: comparison of diffusion- and T2-weighted MRI and spectroscopy. *Magn Reson Med* 1990;14:330-346
10. Chien D, Kwong KK, Gress DR, et al. MR diffusion imaging of cerebral infarction in humans. *AJNR* 1992;13:1097-1102
11. Sorensen AG, Buonanno FS, Gonzalez RG, et al. Hyperacute stroke: evaluation with combined multisection diffusion-weighted and hemodynamically weighted echo-planar MR imaging. *Radiology* 1996;199:391-401
12. Marks MP, de Crespigny A, Lentz D, et al. Acute and chronic stroke: navigated spin-echo diffusion-weighted MR imaging. *Radiology* 1996;199:403-408
13. Gonzalez RG, Schaefer P, Buonanno FS, et al. Diffusion-weighted MR imaging: diagnostic accuracy in patients imaged within 6 hours of stroke symptom onset. *Radiology* 1999;210:155-162
14. Sunshine J, Tarr R, Lanzieri C, Landis D, Selman W, Lewin J. Hyperacute stroke: ultrafast MR imaging of triage patients prior to therapy. *Radiology* 1999;212:325-332
15. Patel MR, Edelman RR, Warach S. Detection of hyperacute primary intraparenchymal hemorrhage by magnetic resonance imaging. *Stroke* 1996;27:2321-2324
16. Atlas SW, Thulborn KR. MR detection of hyperacute parenchymal hemorrhage of the brain. *AJNR* 1998;19:1471-1477
17. Linfante I, Llinas RH, Caplan LR, Warach S. MRI features of intracerebral hemorrhage within 2 hours of symptom onset. *Stroke* 1999;30:2263-2267
18. Clark RA, Watanabe AT, Bradley WG, Roberts JD. Acute hematomas: effects of deoxyhemoglobin, hematocrit, and fibrin-clot formation and retraction on T2 shortening. *Radiology* 1990;174:201-206
19. Hayman LA, Taber KH, Ford JJ, et al. Effect of clot formation and retraction on spin-echo MR images of blood: an in vitro study. *AJNR* 1989;10:1155-1158
20. Hayman LA, Ford JJ, Taber KH, et al. T2 effect of hemoglobin concentration: assessment with in vitro MR spectroscopy. *Radiology* 1988;168:489-491
21. Beall P, Hazlewood C, Rao P. Nuclear magnetic resonance patterns of intracellular water as a function of HeLa cell cycle. *Science* 1976;192:904-907
22. Hargens A, Bowie L, Lent D, et al. Sickle-cell hemoglobin: fall in osmotic pressure upon deoxygenation. *Proc Natl Acad Sci USA* 1980;77:4310-4312
23. Brooks RA, Di Chiro G, Patronas N. MR imaging of cerebral hematomas at different field strengths: theory and applications. *J Comput Assist Tomogr* 1989;13:194-206
24. Bryant RG, Marill K, Blackmore C, Francis C. Magnetic relaxation in blood and blood clots. *Magn Reson Med* 1990;13:133-144
25. Does MD, Zhong J, Gore JC. In vivo measurement of ADC change due to intravascular susceptibility variation. *Magn Reson Med* 1999;41:236-240
26. Schaefer PW. Grant PE, Gonzalez RG. Diffusion-weighted MR imaging of the brain. *Radiology* 2000;217:331-345
27. Thulborn KR, Sorensen AG, Kowall NW, et al. The role of ferritin and hemosiderin in the MR appearance of cerebral hemorrhage: a histopathologic biochemical study in rats. *AJNR* 1990;11:291-297